

Thermodynamics of a tiling model

This article has been downloaded from IOPscience. Please scroll down to see the full text article.

2000 J. Phys. A: Math. Gen. 33 4215

(<http://iopscience.iop.org/0305-4470/33/23/301>)

View [the table of contents for this issue](#), or go to the [journal homepage](#) for more

Download details:

IP Address: 171.66.16.118

The article was downloaded on 02/06/2010 at 08:10

Please note that [terms and conditions apply](#).

Thermodynamics of a tiling model

Luca Leuzzi[†] and Giorgio Parisi[‡]

[†] Instituut voor Theoretische Fysica, Universiteit van Amsterdam, Valckenierstraat 65,
1018 XE Amsterdam, The Netherlands

[‡] Dipartimento di Fisica and INFN, Università di Roma ‘La Sapienza’, P A Moro 2, 00185 Roma,
Italy

Received 8 November 1999, in final form 31 March 2000

Abstract. A specific two-dimensional tiling model, composed of the so-called Wang tiles has been studied at finite temperature using Monte Carlo numerical simulations. In the absence of any thermal bath the Wang tiles provide the opportunity of building a very large number of non-periodic tilings. We can construct a local Hamiltonian such that only perfectly matched tilings are ground states with zero energy. This Hamiltonian has a very large degeneracy. The thermodynamic behaviour of such a system seems to show a continuous phase transition at non-zero temperature. An order parameter with non-trivial features is proposed. Under the critical temperature the model exhibits ageing properties. The fluctuation-dissipation theorem is violated.

1. Introduction to the model

In this paper we present a model that shows a non-trivial thermodynamic pattern of behaviour due to its particular geometric structure.

This two-dimensional model is built using square tiles, called Wang tiles, on a square lattice. The edges of these tiles can be of six different ‘colours’. However, of all the possible types (6^4) that can be created by changing the colours, just one particular group of 16, discovered by Ammann [1], is considered (see figure 1).

This is one of the minimal sets of Wang tiles such that the corresponding tilings exist and are non-periodic. A tiling is a configuration of tiles placed edge to edge on a plane, where all the contiguous edges are the same colour. If at least one tiling is allowed and none of

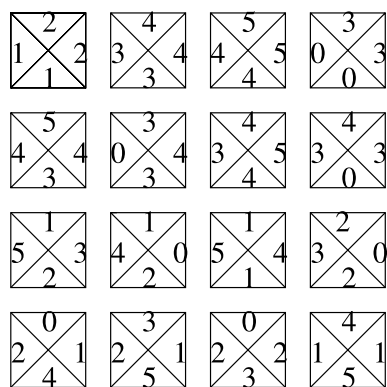


Figure 1. The 16 Wang tiles. The six different types of edges, or ‘colours’ are indicated here by numbers (0, 1, 2, 3, 4, 5). The tiles shown are the minimum set allowing aperiodic tiling.

the possible tilings show a periodic pattern, then the set of tiles composing them is called *aperiodic*. Other aperiodic sets of tiles are often used as models for quasi-crystal materials [2], but not in the present case.

The Wang tiles were the first tiles to be proved aperiodic, in 1966 by Berger [3]. They were initially important, and remain so, because of their use in problems of mathematical logic [1, 4]. However, the use that we make of them in this paper is quite different. We look at the behaviour of a system built by Wang tiles in a thermal bath, defining thermodynamic observables on these tilings. The main stimulus for our study of this model has been the high degeneracy of the perfectly matched configurations and their non-trivial aperiodic structure.

Placing the system in a thermal bath allows for translations of the tiles even in positions where there is no match between the edges of neighbouring tiles, thus forming an unmatched tiling. We can assign an energy to each configuration which is equal to the number of links such that the colours of the facing edges are different. The energy of the exactly matched configurations, which we shall refer to as ground states, is therefore zero.

If we denote the type of tile in the position given by the coordinates (x, y) in the plane by $T_{x,y}$ and the type of its four edges, towards the south, east, north and west by $T_{x,y}^{(S)}$, $T_{x,y}^{(E)}$, $T_{x,y}^{(N)}$ and $T_{x,y}^{(W)}$, respectively, we can write a Hamiltonian for this system as follows:

$$\mathcal{H} = \sum_{(x,y)}^{1,L-1} (1 - \delta(T_{x,y}^{(E)} - T_{x+1,y}^{(W)})) + \sum_{(x,y)}^{1,L-1} (1 - \delta(T_{x,y}^{(N)} - T_{x,y+1}^{(S)})) \quad (1)$$

where L is the number of tiles in the lattice in one direction and $\delta(z)$ is the Kronecker delta function.

2. Equilibrium analysis and critical behaviour

Numerical simulations to study the equilibrium characteristics have been performed using the parallel tempering algorithm [5]. We have chosen open boundary conditions on the two-dimensional lattice. Indeed, using periodic boundary conditions the fact that periodic tilings do not exist would have implied that the energy of the ground state would not have been zero. With open boundary conditions the energy of the ground state is, by definition (1), equal to zero. This is equivalent to saying that all the tiles are edge to edge perfectly matched, forming a non-periodic structure.

2.1. Phase transition

At different temperatures, for every system we have computed the energy and the specific heat. Numerical simulations have been performed on square lattices of different sizes: from a linear size of 8 to one of 32. Every equilibrium simulation has been carried out for a number of Monte Carlo (MC) steps ranging from 10×10^6 to 100×10^6 , relative to the size of the lattice. A range of temperatures between 0 and 5 has been observed, before concentrating at small intervals on what emerges as the critical region, around $T = 0.4$. We checked that at zero temperature the energy goes to zero and that the specific heat computed from the derivative of the energy coincides with that computed from the energy fluctuations. These are the checks of a correct thermalization.

The specific heat presents a smeared but clear change around the temperature 0.4 (see figure 2), from a lower value for lesser temperatures to a higher value for greater ones. On increasing the size of the system, we observe that the crossing points between two curves of

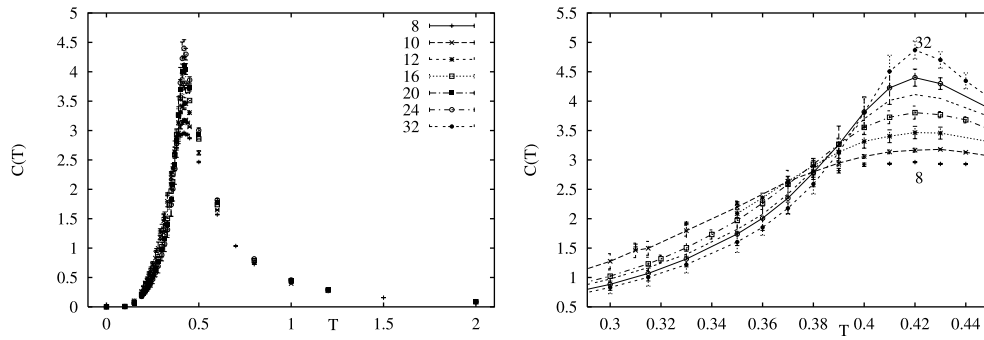


Figure 2. Left, specific heats in the whole probed region. Right, specific heats around the critical region. Linear sizes from 8 to 32 are plotted. The crossing point shifts with the size of the system following a FSS. We can observe both the raising of the slope of the curves around the crossing point and a growing peak at $T = 0.42$.

different size move towards the right and that the slope of the $C_L(T)$ line increases in this interval of temperatures as L increases, but we also see that a peak grows at around $T = 0.42$.

Performing a finite-size scaling (FSS) analysis of the crossing points of the specific heat curves we find that their abscissa tends to a $T_{cross}(\infty) = 0.398 \pm 0.007$ as $L \rightarrow \infty$, with an exponent $\nu = 1.6 \pm 0.5$ and that the behaviour of the slope with increasing size is compatible with a diverging fit at that temperature. In this case we would have a jump at $T_c = T_{cross}(\infty)$, which corresponds to a critical exponent α equal to zero.

However, at the same time the fit of the peak height is consistent with a divergence at $T_c = 0.42 \pm 0.01$. Knowing that at criticality $C \sim |T - T_c|^{-\alpha}$ and $\xi \sim |T - T_c|^{-\nu} \sim L$ we obtain $C \sim L^{\alpha/\nu}$. Our data are both consistent with a power-law divergence ($\alpha/\nu = 0.35 \pm 0.01$), and with a logarithmic one ($\alpha = 0$). A similar value of the critical temperature was found, in this last hypothesis, by Janowsky and Koch [6].

In any case there is evidence for a second-order phase transition.

2.2. Order parameter

Wang's tiles satisfy a particular property: if all the tiles of the two contiguous *west* and *south* sides (or equally of the *north* and *east* sides) of the square lattice are fixed, then at most one aperiodic tiling can be formed. This is due to the fact that each tile of the Wang set has different combinations of west–south (or north–east) colours. Therefore at most only one of them can be put, in the bottom-left (or top-right) corner. The same is true for the tiles to be placed in the two corners created by the placement of the first tile. If any, there will also be only one combination available for them. Of course this is valid at $T = 0$ in our system.

This condition implies that ground state degeneracy cannot increase faster than 16^{2L-1} and therefore the entropy density is zero at zero temperature: $s_L(0) \sim a/L$, where $a < 8 \log 2$. Since only a few north–south or west–east combination are allowed, the actual constant in the entropy is smaller than $8 \log 2$ (a stricter upper bound of $a = \log 12 = 3.585 \log 2$ can be easily obtained).

To identify an order parameter we have to break this degeneracy. We have therefore simulated the parallel evolution of two copies of the system, using the following procedure: one system reaches equilibrium, then a copy of the equilibrium configuration is made and the evolution of this second copy is performed. One fundamental constraint is set: the

boundary tiles on the south and east sides of the lattice stay unchanged in the dynamics towards equilibrium of the second copy.

For $T > 0$ the equilibrium states are no longer the exactly matched tilings. Because of the thermal noise some pair of neighbouring sides of the Wang tiles can be unmatched. Furthermore, there will not be a unique tiling minimizing the energy. The second copy can then evolve to a different configuration.

We are interested in looking at what happens when the temperature is increased from below to above the critical temperature, and how the behaviour is sensitive to the size of the system. With this aim we introduce an *overlap* that depends on the distance l of the tiles from the two contiguous boundary sides that are fixed once the first copy has reached equilibrium:

$$q(l) = \frac{1}{2(L-l)+1} \sum_{y \geq l, x=l} \sum_{x \geq l, y=l} \overline{\langle \delta(T_{x,y}^{(1)} - T_{x,y}^{(2)}) \rangle} \quad (2)$$

where the average $\overline{(\dots)}$ has been performed over different realizations of the configurations, $\langle (\dots) \rangle$ is the time average at equilibrium and $l = 1, \dots, L$.

The overlap $q(l)$ is computed along the diagonal: starting from the vertex shared by the two fixed contiguous sides, $q(1)$, and ending at the opposite vertex of the lattice, $q(L)$. In order to gain more statistics, the overlap is built averaging over the $2(L-l)+1$ elements in the row of ordinate l with the coordinate $x \geq l$ and in the column of abscissa l with $y \geq l$ and assigning this average value to the ‘diagonal’ function $q(l)$.

The statistical sample is formed by repeating the simulation several times with different initial configurations, in order to obtain different equilibrium configurations (we have always checked whether the same equilibrium configuration could possibly appear more than once, starting from different initial configurations in order to avoid annoying biases of the statistical sample, but this has never occurred). Every size has been simulated for at least 100 different initial configurations.

At zero temperature the overlap is always one.

At higher temperatures but below the phase transition, it goes to a constant less than one (far enough from the boundary L , where finite-size effects are overwhelming).

Above the transition point $q(l)$ decays very rapidly, compatible with an exponential, to the lowest possible value, corresponding to completely uncorrelated copies (the *hot* or *disordered* phase). Since the tiles are of 16 different types and the probability distribution of the tile types is uniform, this lowest value is equal to $\frac{1}{16}$.

In figure 3 we show the behaviour of $q(l)$ at different temperatures, both above and below the critical one, for different sizes. From these figures we can see that the $q(l)$ seems to approach some *plateau* for $l \sim L/2$ at temperatures below $T \sim 0.42$. This becomes more evident as we move to bigger sizes.

We can compute a $q(T)$ for every size, averaging over the *plateau* values of $q(l)$. Each time the plateau is chosen taking a small window around $L/2$ and then enlarging it as long as the *plateau* value stays constant. As l grows further finite-size effects destroy this plateau. We observe that this parameter shows a change as it approaches T_c : when $T < T_c$, it increases from the value of $\frac{1}{16}$ that it has at high temperature to the value of 1 that it reaches at zero temperature. The profiles of $q_L(T)$ are plotted in figure 4.

The probability distribution of the values of the overlap at the plateau has a non-trivial shape as soon as $T < T_c$ (figure 5). This is not very surprising since by fixing the boundary conditions we have broken the degeneracy of the equilibrium states. (We stress that due to the definition of the overlap, the distribution does not show any symmetry $q \rightarrow -q$.) The form of the $P(q)$ averaged over different realizations of the tile configurations at two continuous edges

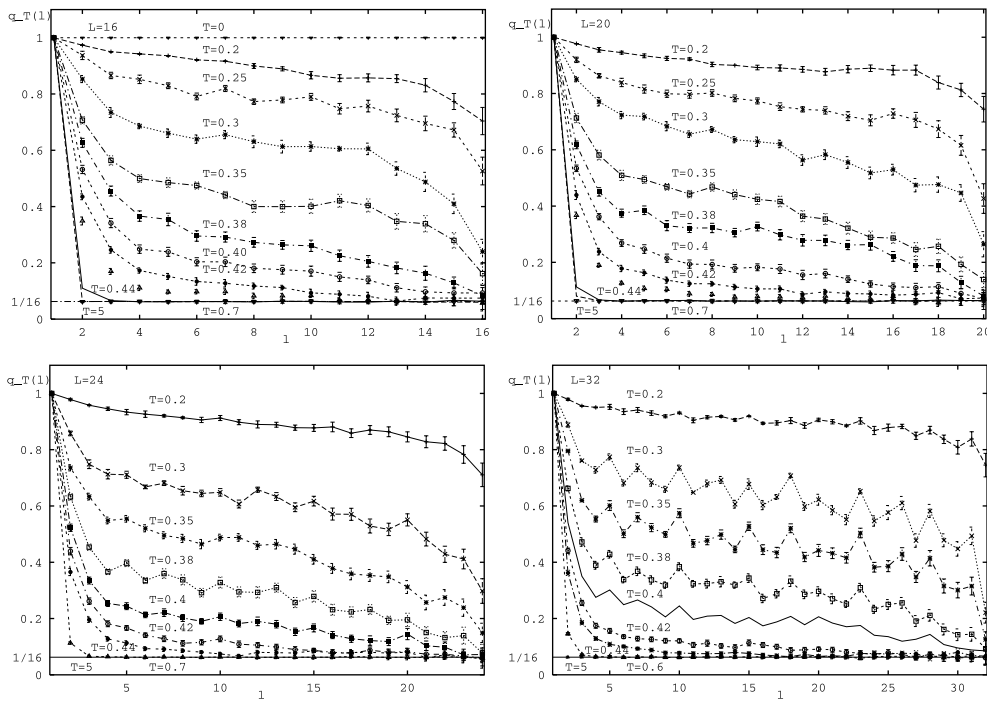


Figure 3. $q_L(l)$ profiles at different temperatures and different sizes. T goes from 0.2 to 5.0 (from top to bottom). The patterns of behaviour for $L = 16, 20, 24, 32$ are shown. For $L = 16$ the pattern of behaviour at $T = 10^{-9}$ is also plotted.

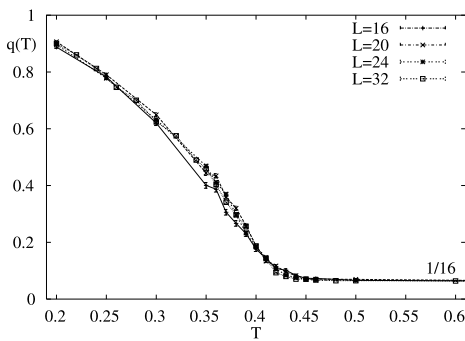


Figure 4. $q_L(T)$ profiles for $L = 16, 20, 24$ and 32 . $q_L(T)$ is the plateau value computed on intervals of three, four, six and ten tiles, respectively.

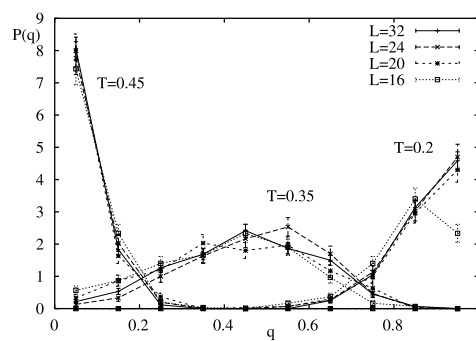


Figure 5. Probability distribution of the overlap values for three different temperature: $T = 0.45$ is already in the disordered phase, while $T = 0.35$ and $T = 0.2$ are under the critical temperature. The behaviour is slightly dependent on temperature. For $T \rightarrow 0$ the distribution tends to a δ function on the value 1.

of the lattice is not strongly dependent on the size of the samples, at least for the simulated cases.

The probability distributions of the overlap for different realizations of the equilibrium boundary conditions in the bottom and left edges of the tiling are represented in figure 6.

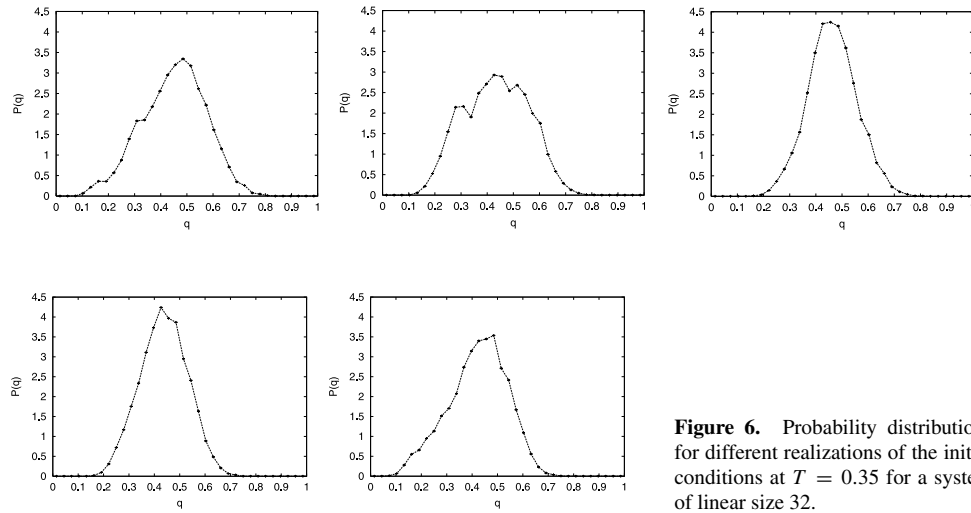


Figure 6. Probability distributions for different realizations of the initial conditions at $T = 0.35$ for a system of linear size 32.

3. Off-equilibrium analysis

In order to study systems with very slow relaxation times, much greater than the experimental times, it is very important to look at the off-equilibrium dynamics. This approach describes glasses, spin glasses and, in general, any system with many equilibrium states divided by high free energy barriers, in a more realistic way than an equilibrium approach, since equilibrium is, in practice, never reached during experiments.

To keep the sample out of equilibrium during the running of a numerical simulation we need the typical distance $\xi(t)$ over which the system has reached equilibrium at a certain time to be always smaller than the linear size L of the lattice. This distance is also called the *dynamical correlation distance*. For practical reasons, in order to be sure of avoiding thermalization, we choose sizes bigger than those used in the static analysis. The greater the size the longer is the time needed for the correlation distance to reach the size of the system. Moreover, in this case we used a standard Monte Carlo algorithm instead of the parallel tempering, so that the thermalization times increased sensitively under the transition point.

In order to study the response of the system to an external field we can embed the system into a perturbative field. Namely a field directed in one of the 16 possible directions in the ‘tile-types space’, where a particular tile of the set of 16 can be favoured (positive field) or disfavoured (negative field). This can be a uniform or non-uniform field. To avoid any preference towards one particular type of tile we have chosen a non-uniform random field, whose value at each site is independent from the other sites.

Thus we add to the Hamiltonian (1) the perturbative term

$$\sum_{(x,y)} h_{x,y}^{sign} (1 - \delta(T_{x,y} - h_{x,y}^{type})) \quad (3)$$

where $h_{x,y} = h_{x,y}^{type} h_{x,y}^{sign}$ is the random external field pointing along one of the tile types or opposite to it.

$h_{x,y}^{type}$ has a uniform distribution of the 16 possible choices of tile type, and $h_{x,y}^{sign}$ gives the magnitude of the field and its sign (it can be randomly positive or negative, always according to a uniform distribution).

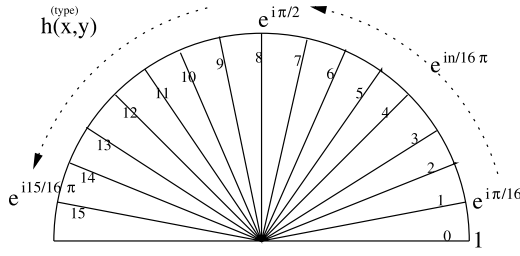


Figure 7. ‘Directions’ of the random field h^{type} in the space of tile types, represented in the complex plane.

The probability distribution can then be written as

$$\mathcal{P}(h_{x,y}) = \frac{1}{16} \sum_n^{0,15} \delta(h_{x,y}^{type} - e^{i\pi n/16}) \times \frac{1}{2} (\delta(h_{x,y}^{sign} - h_o) + \delta(h_{x,y}^{sign} + h_o)) \quad (4)$$

with $\overline{h_{x,y}} = 0$ and $\overline{h_{x,y}^2} = h_o^2$, $n = 0, \dots, 15$ gives the ‘direction’ of the field in a representation in the complex plane (see figure 7)

Once the system has cooled from a high temperature, it is left evolving until a certain time t_w , usually called *waiting time*. At $t = t_w$ the field is switched on and we begin recording the values of the temporal correlation function $C(t, t_w)$ and of the integrated response function $m(t, t_w)$.

For our model they are defined as follows:

$$C(t, t_w) = \frac{1}{L^2} \sum_{x,y} \delta(T_{x,y}(t) - T_{x,y}(t_w)) \quad (5)$$

$$m(t, t_w; h) = \frac{1}{L^2} \sum_{x,y} \frac{\overline{\langle h_{x,y}^{sign}(t_w) \delta(T_{x,y}(t) - h_{x,y}^{type}(t_w)) \rangle}}{h_o} \quad (6)$$

and the susceptibility is

$$\chi(t, t_w) = \lim_{h_o \rightarrow 0} \frac{m(t, t_w; h)}{h_o}. \quad (7)$$

For numerical computation it becomes

$$\chi(t, t_w) \sim \frac{m(t, t_w; h)}{h_o}. \quad (8)$$

Here $\langle \dots \rangle$ is the average over different dynamical processes and $\overline{\langle \dots \rangle}$ the average over the random realizations of the perturbative external field. In a system at equilibrium the fluctuation–dissipation theorem (FDT) holds

$$\chi(t - t_w) = \frac{1 - C(t - t_w)}{T} \quad (9)$$

where we have made explicit use of the fact that the correlation function is defined in such a way that $C(t_w, t_w) = C(0) = 1$.

Out of equilibrium this theorem is no longer valid. However, a generalization is possible [7], at least in the early times of the dynamics. This generalization is made by introducing a multiplicative factor $X(t, t_w)$ depending on two times such that

$$\chi(t, t_w) = \frac{X(t, t_w)}{T} (1 - C(t, t_w)). \quad (10)$$

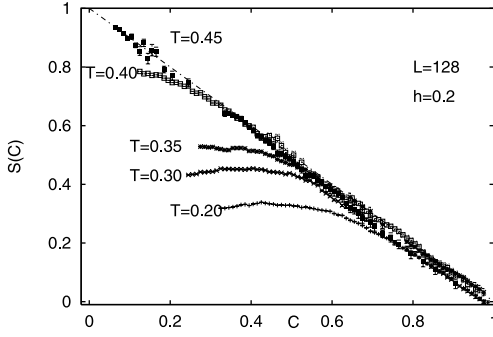


Figure 8. $L = 128$, $h = 0.2$, $S[C]$ at different temperatures. $T = 0.45$ is above the phase transition: in this case there is no regime in which the fluctuation-dissipation theorem does not hold. The time evolution of the system for $t \geq t_w$ has to be read going from right ($C(t_w, t_w) = 1$) to left.

In a certain regime, called the *ageing* regime, $X(t, t_w) < 1$ and the FDT is violated. An important assumption is that this modified coefficient $X(t, t_w)/T$ depends on t and t_w only through $C(t, t_w)$. Its inverse is also called *effective temperature* $T_e \equiv T/X[C(t, t_w)]$ since the system in this regime, for a given time-scale, seems to behave like a system in equilibrium at a temperature which differs from the heat-bath temperature.

In terms of susceptibility and correlation functions we can write the following general functional dependence:

$$\chi(t, t_w) = \frac{1}{T} S[C(t, t_w)]. \quad (11)$$

The $S[C]$ here defined would be $1 - C$ if we were at equilibrium.

From our probe we find that we first have a regime where the relation is linear with a coefficient equal to the heat-bath temperature. This early regime is sometimes called *stationary*, since the observables computed at very short times (compared with t_w) do not depend on the age of the system. During this regime the system goes quickly towards a local minimum.

After this initial time the $S[C]$ bends and the coefficient of $X(t, t_w)/T$ is no longer the inverse heat-bath temperature. $X(t, t_w)$ is now less than one, as if the system were at an effective temperature higher than that of the heat bath. It also seems to change continuously as the system evolves, until it reaches zero (figures 8–10).

The value of the autocorrelation function at which $S[C]$ leaves the $1 - C$ line, equal to the average overlap value q in the static, increases continuously with temperature, as we already observed in the static analysis.

The $S[C]$ shows no strong dependence on the magnitude of the field, at least for the values that we have used to perturb the system. Furthermore, the system shows only a slight dependence on the size (measures on $L = 64, 128, 256$) (figure 9).

From figures 10 we can see that $S[C]$ moves towards some asymptotic line increasing t_w .

The initial difference between $1 - C$ and $S[C]$ results from a lack of statistics: if N_{fr} is the number of field realizations performed in the simulation there is a difference of order N_{fr}/L^2 between the value of the integrated response function in the thermodynamic limit and the value at finite size.

We can also look at the link with the static analysis. As in the case of mean-field spin glasses we can suppose, following [8, 9], that for $t, t_w \rightarrow \infty$, $C(t, t_w) \rightarrow q$ and $X[C(t, t_w)] \rightarrow x(q)$, where $x(q)$ is the cumulative distribution of $P(q)$:

$$x(q) = \int_0^q dq' P(q'). \quad (12)$$

If this link is valid we can connect the susceptibility multiplied by the heat-bath temperature at a certain correlation value ($S[C]$) to the integral $\int_1^C dq x(q)$.

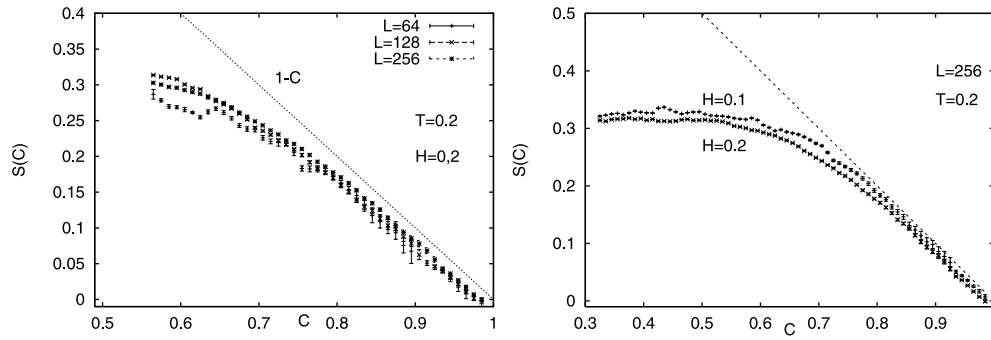


Figure 9. Left, $T = 0.2, h = 0.2, S[C]$ for different sizes. The dependence on the size is small. Right, $L = 256, T = 0.2, S[C]$ for different values of h .

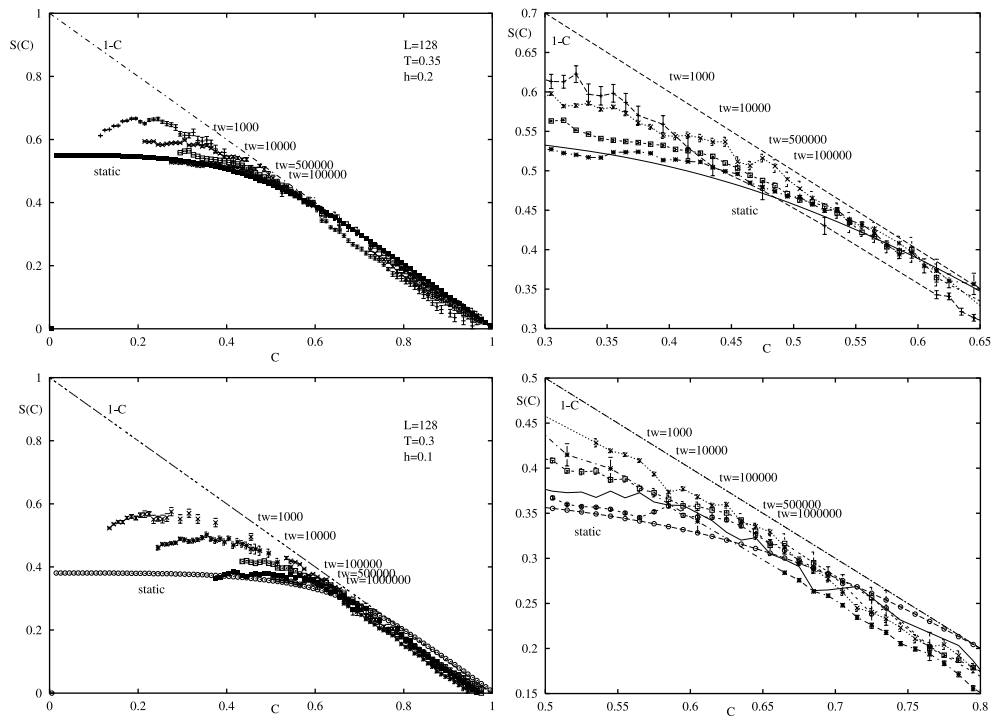


Figure 10. Comparison between $S[C]$ computed on dynamic and static data. The *static* curve is computed from the data of a system of linear size $L = 32$ at equilibrium. The other curves are from the data of a system with 128×128 tiles out of equilibrium. Measurements starting at different waiting times t_w are shown. The two plots above represent the situation at $T = 0.35$, where a perturbative external field of magnitude $h_o = 0.2$ has been applied at t_w . The two below show the relation between response and correlation functions at $T = 0.30$, with $h_o = 0.1$. For large t_w the dynamically determined $S[C]$ tend to lay on the asymptotic *static* curve. On the right-hand side plots of the detail of the beginning of the bending are shown.

In our case there is an agreement between the dynamic data and the values of this last integral computed on the static data. The two approaches are consistent if the external field is not too large, in order to avoid the nonlinear effects that are neglected in the derivation of

formula (6). However, the field also cannot be too small, in order to make the system move from the metastable state into which it has gone during t_w . The lower the temperature at which we cool the system, the bigger is the external field required to make it explore other parts of the space of states. A probe at too low a temperature, therefore, does not really work because nonlinear effects interfere heavily or because the system does not reach the ageing regime.

Two examples of the agreement between dynamic and static data are shown in figure 10.

4. Conclusions

We have studied the thermodynamics of a tiling model built of Wang tiles. For this kind of system we have found evidence of a phase transition from a completely disordered phase, in which the tiles on the plane are completely uncorrelated to each other, to a phase in which they begin to present an organized, albeit a very complicated, structure. For $T \rightarrow 0$ this structure becomes an exactly matched tiling.

In order to characterize the phase of the system we have determined an order parameter with a non-zero mean value below T_c . It is the overlap between two tilings built with the same boundary conditions on the lower and the left-hand sides of the lattices. Our data hint that it could have a non-trivial probability distribution under the phase transition.

Under the critical point the tiling system displays the ageing phenomenon: the response of the system to an external perturbation and the time autocorrelation function depend on the history of the system. This leads to a violation of the fluctuation–dissipation theorem for $T < T_c$. The integrated response function multiplied by the temperature ($S[C]$) shows a progressive bending when the system leaves the stationary regime until it reaches a constant value ($X = 0$) and the dynamically and statically determined q values increase continuously with decreasing temperature.

From this kind of behaviour it is not clear whether the model belongs to the class of systems showing domain growth or whether it is rather more similar to a spin glass in a magnetic field. Indeed, for very long times (small values of the correlation function) the fluctuation–dissipation ratio goes eventually to zero and we cannot rule out that the dynamics evolves through domains growth [10], even though in our case the nature of the domains of tiles should still be theoretically understood. Nevertheless, for a very large interval of time, i.e. values of C in the plot of figure 10, the $S(C)$ is continuously bending ($0 < X < 1$) as in a spin-glass model [9, 11], especially in the regions $0.3 < C < 0.6$, for $T = 0.35$, and $0.4 < C < 0.7$, for $T = 0.3$, as shown in figure 10. For values of C smaller than these the $S(C)$ curves flatten but the predictions obtained from the static behaviour (the $P(q)$ shown in figure 5) are also nearly flat, making it quite difficult to distinguish between a domain growth dynamics, where the response function is constant in the ageing regime, and a more complicated pattern of behaviour where even the response function shows ageing.

Finally, we show that our data are consistent with the equivalence between the equilibrium function $\int_C^1 dq x(q)$ and the dynamically determined $S[C]$ as $t, t_w \rightarrow \infty$.

Acknowledgment

We warmly thank J Kurchan for having stimulated this work and for his advice.

References

- [1] Gruenbaum B and Shephard G C 1987 *Tilings and Patterns* (New York: Freeman)
- [2] Shechtman D, Blech I, Gratias D and Cahn J W 1984 *Phys. Rev. Lett.* **53** 1951
Levine D and Steinhardt P J 1984 *Phys. Rev. Lett.* **53** 2477
Oxborrow M and Henley C L 1993 *Phys. Rev. B* **48** 6966
Henley C L 1998 *J. Phys. A: Math. Gen.* **21** 1649
- [3] Berger R 1966 The undecidability of the domino problem *Mem. Am. Math. Soc.* no 66
- [4] Kari J 1996 A small aperiodic set of Wang tiles *Discrete Math.* **160** 259–64
Culik K II and Kari J 1997 On aperiodic sets of Wang tiles *Found. Comput. Sci.: Potential Theory Cogn.* p 153
- [5] Hukushima K and Nemoto K 1996 *J. Phys. Soc. Japan* **65** 1604–8
- [6] Koch H Private communication
- [7] Bouchaud J P, Cugliandolo L, Kurchan J and Mezard M 1996 *Physica A* **226** 243
- [8] Cugliandolo L and Kurchan J 1993 *Phys. Rev. Lett.* **71** 173
Franz S and Mezard M 1994 *Europhys. Lett.* **26** 209
Franz S, Mezard M, Parisi G and Peliti L 1998 *Phys. Rev. Lett.* **81** 1758
- [9] Marinari E, Parisi G, Ricci-Tersenghi F, Ruiz Lorenzo J J 1998 *J. Phys. A: Math. Gen.* **31** 2611
- [10] Barrat A 1998 *Phys. Rev. Lett.* **51** 3629
Berthier L, Barrat J-L and Kurchan J 1999 *Eur. Phys. J. B* **11** 635
- [11] Parisi G, Ricci-Tersenghi F, Ruiz Lorenzo J J 1999 *Eur. Phys. J. B* **11** 317